DENSITY MODELS FOR THE UPPER ATMOSPHERE*

DOUGLAS L. DOWD

Aerospace Engineer, Mission Planning and Analysis Division, LBJ Space Center, Houston, Tex., U.S.A.

and

B. D. TAPLEY

Professor, Department of Aerospace Engineering and Engineering Mechanics, The University of Texas at Austin, Austin, Tex., U.S.A.

(Received 12 December, 1978; accepted 19 January, 1979)

Abstract. Modeling the effects of atmospheric drag is one of the more important problems associated with the determination of the orbit of a near-earth satellite. Errors in the drag model can lead to significant errors in the determination and prediction of the satellite motion. The uncertainty in the drag acceleration can be attributed to three separate effects: (a) errors in the atmospheric density model, (b) errors in the ballistic coefficient, and (c) errors in the satellite relative velocity. In a number of contemporary satellite missions, the requirements for performing the orbit determination and predictions in near real-time has placed an emphasis on density model computation time as well as the model accuracy. In this investigation, a comparison is made of three contemporary atmospheric density models which are candidates for meeting the current orbit computation requirements. The models considered are the analytic Jacchia–Roberts model, the modified Harris–Priester model, and the USSR Cosmos satellite derived density model. The computational characteristics of each of the models are compared and a modification to the modified Harris–Priester model is proposed which improves its ability to represent the diurnal variation in the atmospheric density.

1. Introduction

One of the more important problems associated with the task of defining the orbit of a near earth satellite is that of modeling the effects of atmospheric drag. Errors in the drag model can lead to significant errors in the determination and prediction of the satellite position. The drag acceleration is modeled by the relation

$$\mathbf{A}_D = -\tfrac{1}{2}\rho C_D \frac{A}{m} V_r \mathbf{V}_r, \tag{1}$$

where ρ is the atmospheric density, C_D is the drag coefficient, A is the cross sectional area normal to the relative velocity vector, m is the satellite mass, and $\mathbf{V}_r$ is the velocity vector relative to the atmosphere. Hence, the uncertainty in the drag acceleration can be attributed to three separate effects: (a) errors in the atmospheric density model, (b) errors in the ballistic coefficient model, and (c) errors in the satellite relative velocity. The first of these error sources, which is due to inaccuracies in the models used to define the atmospheric density, is a limiting factor in the accuracy with which the position and velocity of many current earth orbiting satellites can be determined.

* This investigation was supported by the NASA Goddard Spaceflight Center under contract NAS5-20946 and Contract NSG 5154.

Celestial Mechanics **20** (1979) 271–295. 0008–8714/79/0203–0271$03.75.
Copyright © 1979 by D. Reidel Publishing Co., Dordrecht, Holland and Boston, U.S.A.

Normally, the atmospheric density is determined by using an a-priori model based on historical satellite tracking data. Since the atmospheric density depends on such time varying external influences as solar and geomagnetic activity, computed values of the density will be in error due to inaccuracies in the original definition of the density model as well as time lags in updating the parameters which account for the effects of solar and geomagnetic activity.

In a number of contemporary satellite missions, the requirement for performing the orbit determination and prediction in near real-time has placed an emphasis on models which, in addition to being accurate, require a minimum of computation time. Furthermore, if the computations are to be performed using a satellite-borne computer, the model must be efficient with regard to computer storage requirements.

In this investigation, consideration is given to three contemporary atmospheric density models which are the best candidates for meeting these requirements. The models considered are the Analytic Jacchia–Roberts Model [1], the Modified Harris–Priester Model [2], and the U.S.S.R. Cosmos Satellite Derived Density Model, commonly known as either the Russian Model or the U.S.S.R. Model [3]. Each of the models, as well as several variations of the basic models is discussed separately, and a comparison of their computational characteristics is made.

2. The Analytic Jacchia–Roberts Model

The Analytic Jacchia–Roberts Model calculates atmospheric densities for altitudes at 90 km and above [1]. This model is an analytic representation of Jacchia's 1970 tabular density model [4]. As developed by Roberts [1], it incorporates the revisions to the 1970 model which were published by Jacchia in 1971 [5]. The model divides the upper atmosphere into three altitude bands for calculation of the atmospheric density. Specifically, these bands are 90–100 km, 100–125 km, and higher than 125 km. The terminal conditions in each lower band are the initial conditions for the next higher band. Therefore, the determination of the density within any given altitude band requires the calculation of the terminal conditions in each of the lower bands. The model is developed by adopting a specific temperature profile as well as assuming values for the molecular mass of the major atmospheric constituents. The atmospheric density is determined then by integrating either the barometric equation for altitudes from 90 km to 100 km or the diffusion equation for altitudes above 100 km. The major constituents considered by Jacchia are nitrogen (N_2), argon (Ar), helium (He), molecular oxygen (O_2), atomic oxygen (O), and hydrogen (H).

For altitudes in excess of 125 km, Jacchia originally assumed an inverse tangent function for the temperature profile. This assumption does not produce an exact differential in the diffusion equation and the Jacchia model is obtained by numerically integrating the diffusion equation. Roberts [1] assumed an exponential temperature profile which allows for the analytic integration of the diffusion equation. In either of the assumed temperature profiles, there is no mathematical upper altitude limit. As altitude increases without bound, the temperature asymptotically

approaches the exospheric temperature. At some unspecified altitude, the density of the atmosphere has decreased to the point where the gas atoms move in ballistic trajectories and no longer interact with one another in support of the laws of fluid dynamics. Therefore, as the temperature profile approaches its bound, the applicability of the diffusion equation becomes suspect. The altitudes at which this occurs in the model is highly dependent upon the value of the exospheric temperature [5] and ranges from 880 km for an exospheric temperature of 500 K, to 2000 km at 1900 K.

In the original Jacchia model, and in the analytic model as well, the exospheric temperature (T_∞) accounts for the temporal variations in the density. The variations in T_∞ are correlated both with variations in the 90-day mean flux of the solar 10.7 cm radiation, $\bar{F}_{10.7}$, and with $F_{10.7}$, the daily flux which varies in a random fashion from the mean. The value of the solar flux varies with an 11-year period while the $F_{10.7}$ flux has a 27-day period with an apparently random amplitude due to the effects of the solar rotation. The temperature calculation also accounts for the variation in density as a function of the local solar time (diurnal effect) and changes in the geomagnetic activity. The atmospheric density determined from this exospheric temperature is corrected for the seasonal-latitude variations of helium, and the variations in hydrogen concentrations above 500 km. A simple logic flow chart of the Analytic Jacchia–Roberts Model is shown in Figure 1 while the specific algorithm for the atmospheric density model is described in detail in [6].

An efficient modification to the basic Jacchia–Roberts Model has been adopted for use in the Goddard Trajectory Determination Subsystem (GTDS) [2]. In the essential modifications, the atmospheric density at 100 km and the density numbers of the major atmospheric constituents at 125 km are approximated by sixth degree polynomials in T_∞ instead of being calculated using the terminal conditions of the two lowest altitude boundaries. The computational aspects of these modifications are discussed in Section 6.

3. The Modified Harris–Priester Model

The Modified Harris–Priester Model [2] is based on an extensive tabular static model of the upper atmosphere in the altitude band from 120 km to 800 km [7]. In the first modification of the Harris–Priester Model, accomplished at the NASA Goddard Space Flight Center, the tables were extrapolated exponentially to include altitudes down to 100 km and up to 1000 km [2]. In the original Harris–Priester Model, there are ten separate tables, each associated with a particular value of the smoothed (5-month average) flux of the solar 10.7 cm radiation ranging from $\bar{F}_{10.7} = 65$ to $\bar{F}_{10.7} = 275$. This range of $\bar{F}_{10.7}$ encompasses the total variation of $F_{10.7}$ over the 11-year solar cycle. Each table is divided into twelve subtables which list the atmospheric densities for the local solar time at 2-hr intervals. The tables for the Modified Harris–Priester Model are formed by extracting the maximum and the minimum densities for each altitude from the subtables for each solar flux level. The

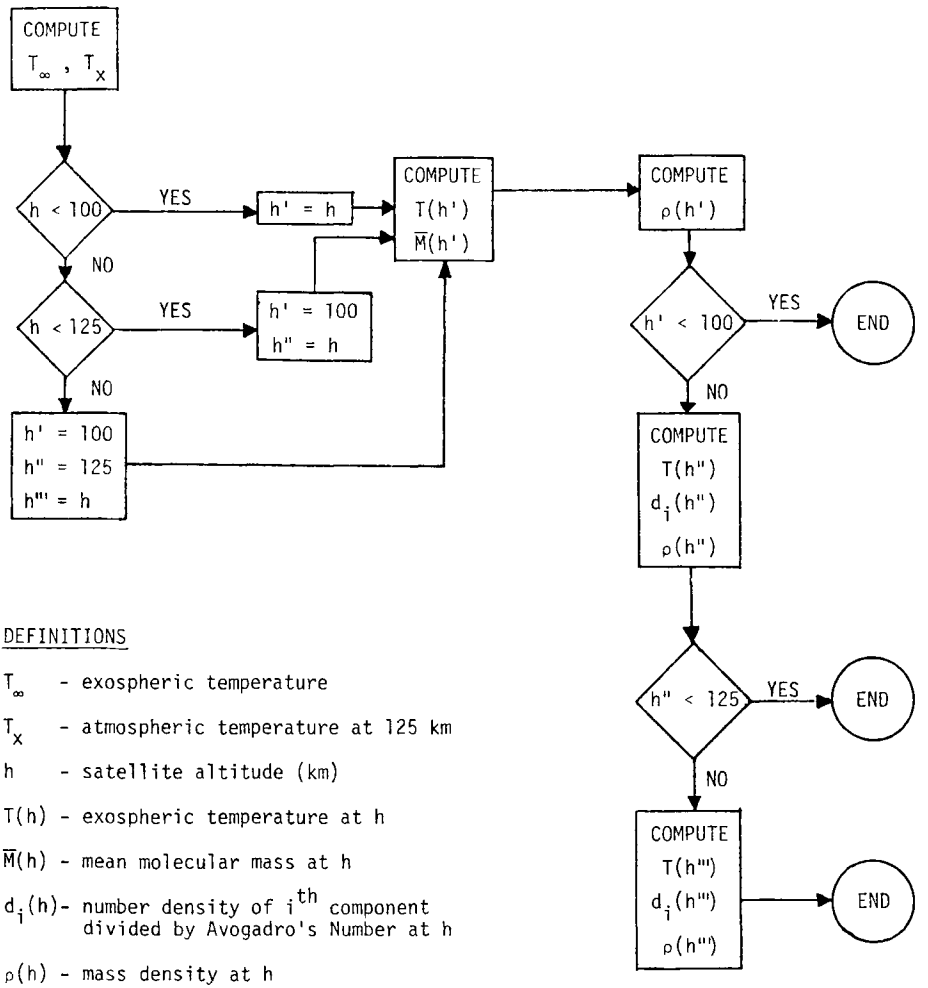

Fig. 1. Logic flow chart for analytic Jacchia–Roberts Model.

absolute maximum and minimum are chosen without regard for the local solar time. This procedure was adopted because the diurnal maximum and minimum densities do not appear in the tables at 1400 hr and 0400 hr at altitudes below 320 km. The Modified Harris–Priester Model then derives the atmospheric density from a set of ten tables associated with the smoothed flux of the 10.7 cm solar radiation, where each table relates a diurnal maximum and minimum density for each of the tabulated altitudes from 100 to 1000 km.

The atmospheric density for a given altitude is determined by entering the table associated with the value of $\bar{F}_{10.7}$ most nearly equal to the measured solar flux, exponentially interpolating the maximum and minimum densities with respect to altitude, and then applying a cosine interpolation for the diurnal variation. This procedure yields a density distribution which is symmetric with respect to the apex of

the diurnal bulge. The apex of the diurnal bulge is assumed to follow the subsolar point by 30° in the same latitude. It is known [8] that the observed diurnal variation is not symmetric and the Analytic Jacchia–Roberts [1] and the U.S.S.R. Cosmos Satellite Derived [3] models account for the asymmetry. The Jacchia–Roberts Model models this effect by computing an asymmetric temperature distribution from which the density is determined. In this investigation, a similar procedure has been applied directly to the density computation to obtain an asymmetric density distribution for the Modified Harris–Priester Model. The model, which results when this procedure is adopted, is referred to as the Asymmetric Modified Harris–Priester Model. The detailed computational algorithms are given in [6].

The pertinent equations for describing the diurnal variation in the Modified and Asymmetric Modified Harris–Priester Models are as follows:

Modified Harris–Priester Model

$$\rho(h) = \rho_{\min}(h) + [\rho_{\max}(h) - \rho_{\min}(h)] \cos^n (\psi/2) , \tag{2}$$

where h is the altitude, $\rho_{\min}(h)$ and $\rho_{\max}(h)$ are the interpolated daily minimum and maximum densities from the modified tables [2], and ψ is the angle between the geocentric position vectors of the point where the density is desired and the apex of the diurnal bulge.

Asymmetric Modified Harris–Priester Model

$$\rho(h) = \rho_N(h) + [\rho_D(h) - \rho_N(h)] \cos^n (\tau/2) , \tag{3}$$

where

$$\begin{aligned} &\rho_N(h) = \rho_{\min}(h) + [\rho_{\max}(h) - \rho_{\min}(h)] \sin^m \theta , \\ &\rho_D(h) = \rho_{\min}(h) + [\rho_{\max}(h) - \rho_{\min}(h)] \cos^m \eta , \\ &\theta = \tfrac{1}{2}|\phi + \delta| , \\ &\eta = \tfrac{1}{2}|\phi - \delta| , \\ &\tau = H + \beta + \lambda \sin (H + \gamma) , \qquad (-\pi \leqslant \tau \leqslant \pi) . \end{aligned} \tag{4}$$

In the above equations, H is the local solar time, ϕ is the geographic latitude of the subsatellite point, and δ is the solar declination. The values for the parameters appearing in Equations (4), taken from Jacchia's temperature equation [5], are:

$$\begin{aligned} &m = 2.2 , \qquad \beta = -37° , \qquad \gamma = 43° , \\ &n = 3 , \qquad \lambda = 6° . \end{aligned}$$

The qualitative shape of the diurnal bulge, as modeled by the Asymmetric Modified Harris–Priester Model, is illustrated in the polar plots in Figures 2 and 3. In Figure 2, the angle measure, ϕ, is latitude, and the magnitude in the radial direction

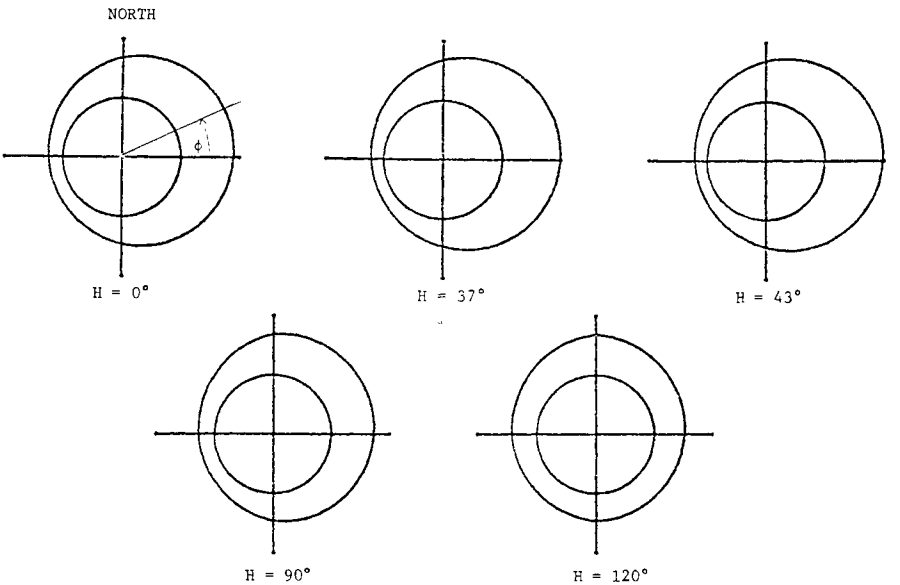

Fig. 2. Latitudinal density profile variation with solar hour angles, H.

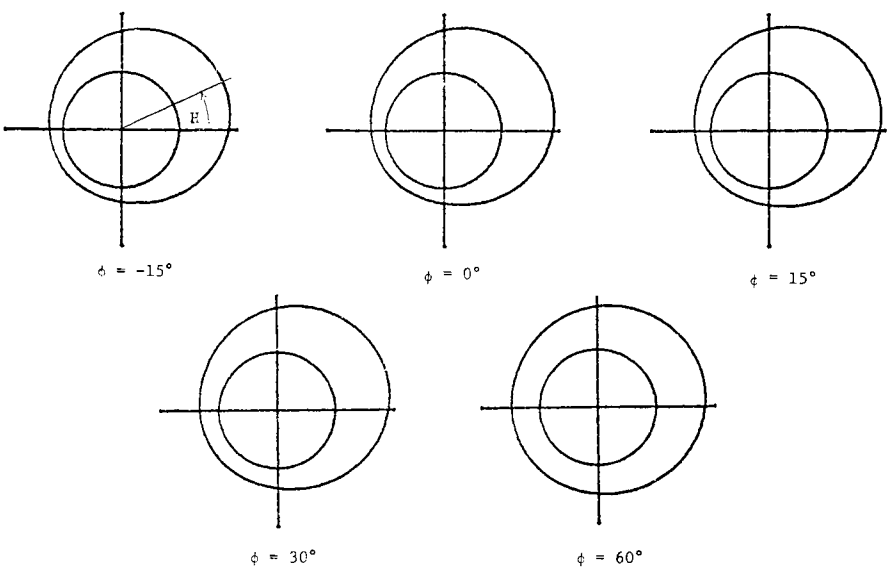

Fig. 3. Longitudinal density profile variation with latitudes, ϕ.

represents the normalized modeled density variation at some assumed constant altitude h where $\rho_{\min}(h) = 1.2$ and $\rho_{\max}(h) = 2.0$ are the assumed density values at h. The specified solar hour angles H are for the right halves of the plots with the hour angle for the left halves being $H + 180°$. In Figure 3, the angle measure is longitude (or solar hour angle) measured from noon, and the radius magnitude represents the

modeled variation at constant altitude and latitude. In both Figures 2 and 3, the assumed solar declination is 15°. The unit circles in each figure are included to emphasize the changes in the density magnitude. Both Figures 2 and 3 show the global maximum density occurring at the subsolar latitude ϕ_δ and 31.226° after noon and the global minimum occurring at latitude $-\phi_\delta$ and 137.01° before noon. This variation closely approximates the density variation associated with the Jacchia atmosphere model.

4. The U.S.S.R. Cosmos Satellite Derived Density Model

The U.S.S.R. Cosmos Satellite Derived Density Model is based on the observations of 145 Cosmos satellites over the time period from 1964 through 1970 [4]. The model determines the atmospheric density directly by substituting the input parameters into a set of equations containing twenty coefficients derived by fitting density observations over the range of altitudes and temperatures encountered by the Cosmos satellites. The use of the current model is restricted because the coefficients were empirically determined over a limited altitude region and during only a portion of the 11-year solar cycle. The data were extended by using Jacchia's 1970 Model, but the altitudes for which the model is valid is still only between 140 and 500 km. The coefficients are given in four sets for four reference values F_0 of the 10.7 cm solar radiation flux; specifically, 75, 100, 120, and 150×10^{-22} W m^{-2} Hz^{-1}. Since the model uses the reference value F_0 which is nearest the 6-month average of the daily $F_{10.7}$, the model is valid for 6-months averages of $F_{10.7}$ between 65 and 165×10^{-22} W m^{-2} Hz^{-1}.

The details of the U.S.S.R. Model are given in [6]. The essence of the model is that the nighttime density profile ρ_h is corrected by four multiplicative factors K_i, $i = 1, 2, 3, 4$. The K_i-factors include corrections for the diurnal density variation, K_1, the daily variation of $F_{10.7}$, K_2, the observed semi-annual variation in density, K_3, and fluctuations in geomagnetic activity, K_4.

The total density is then represented by the equation

$$\rho = \rho_h K_1 K_2 K_3 K_4 . \tag{5}$$

5. Explanation of Atmospheric Density Profiles

A study of atmospheric density and its effect on the motion of a near-earth satellite would not be complete without an explanation of the correlation between the orbit of the satellite and the density profile which is encountered by the satellite. Normally, the atmosphere is discussed as a separate system with density presented as a function of altitude for various values of the other parameters which have been correlated to variations in the observed densities. In this discussion, the intersection and interaction of two dynamical systems, the atmosphere and the orbiting satellite, will be considered. The density profiles which will be discussed are referred to the Modified

Analytic Jacchia–Roberts Model since this model contains all of the essential variations while retaining computational efficiency.

It is not difficult to understand the relationship between atmospheric density and altitude – as altitude above the Earth's surface increases, density decreases, provided everything else is constant. Therefore, one would expect to see the atmospheric

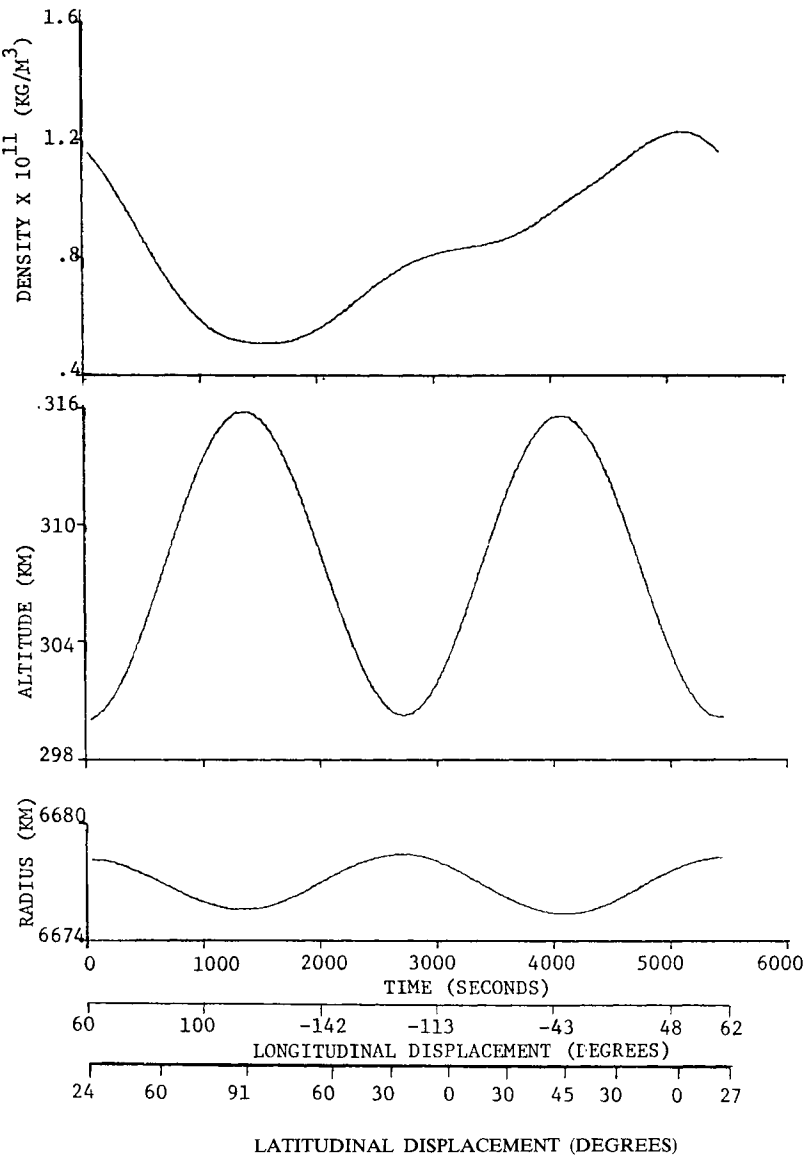

Fig. 4. Density profile ($\Omega = 0°$).

density vary inversely to the variation of the satellite altitude as it moves in its orbit. Obviously, orbital eccentricity has a large effect on the altitude variation. Considering that the Earth is not spherical, orbital inclination also has an influence on the altitude variation as does the orbital perturbations due to the non-sphericity of the geopotential. To illustrate these points, refer to Figure 4, which shows time histories of altitude above the reference ellipsoid, geocentric radius and atmospheric density for one orbital period. The orbit used to generate these results is approximately circular with initial osculating Keplerian elements as follows:

$a = 6\,682\,473$ m

$e = 0.000\,646\,254$

$i = 67.99°$

$\omega = 0.0°$

$\Omega = 0.0°$

$E = 0.0°$

epoch $16^{d}2^{h}47^{m}\ 55.537^{s}$ December 1973.

It should be noticed that the amplitudes of the variations in radius and in altitude are not of the same magnitude, a fact which indicates the dual effect of the Earth's nonsphericity on the altitude variation and, in turn, on the density profile. The density curve indicates that there are other major effects in shaping the density profile. To aid in the identification of the most obvious of these effects, consider the histograms in Figure 5, which were generated exactly as those in Figure 4 except that the nodal line has been rotated 90°, i.e., $\Omega = 90°$. The altitude variation and latitudinal displacement from the diurnal bulge are the same in both cases, whereas the longitudinal displacement from the diurnal bulge is offset by 90°. There is a marked difference in the density profile which appears as a phase shift in an apparent once-per-revolution variation. This difference illustrates the diurnal variation and its relative importance in modeling atmospheric density.

Up to this point the discussion has related to the shape of the density profile. The magnitude of the atmospheric density exhibits other variations which are still present when altitude and diurnal variations are eliminated. Most significant are the variations in density due to variations in solar radiation and the interaction of the solar wind with the Earth's magnetic field. Density profiles are presented in Figures 6 through 8 which illustrate the changes in density that are correlated with both long and short term variations in solar extreme ultraviolet (EUV) radiation, as evidenced by the flux of the 10.7 cm solar radiation for a value $K_p = 1$. The effects of geomagnetic heating on the magnitude of density are shown in Figure 9 in which density profiles are presented for four values of the planetary geomagnetic index K_p. The initial conditions used to generate the orbits for Figures 6 through 9 are the same as those used for Figure 4.

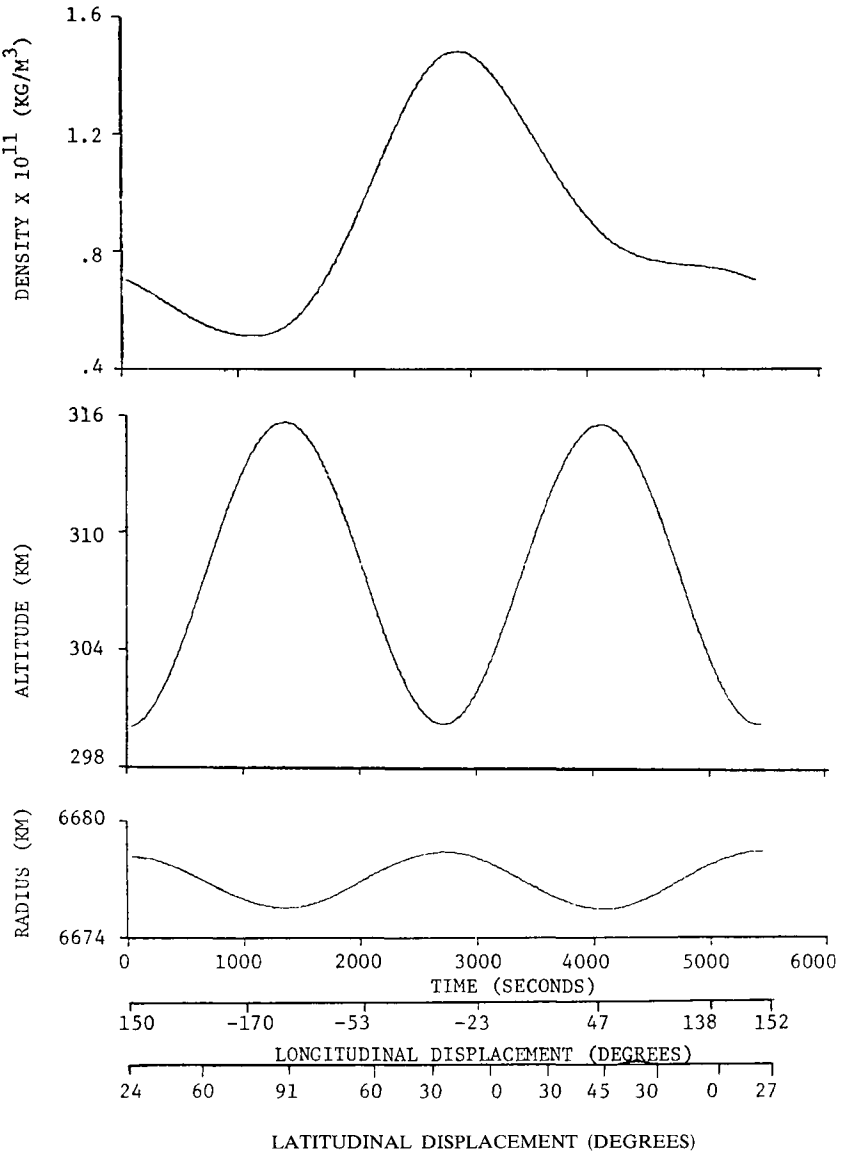

Fig. 5. Density profile ($\Omega = 90°$).

6. Comparison of the Density Models

Each of the density models discussed in the preceding sections will yield a density profile along any given trajectory which is different than the density computed by any other model. Comparisons of the density profiles are shown pictorially in curves of

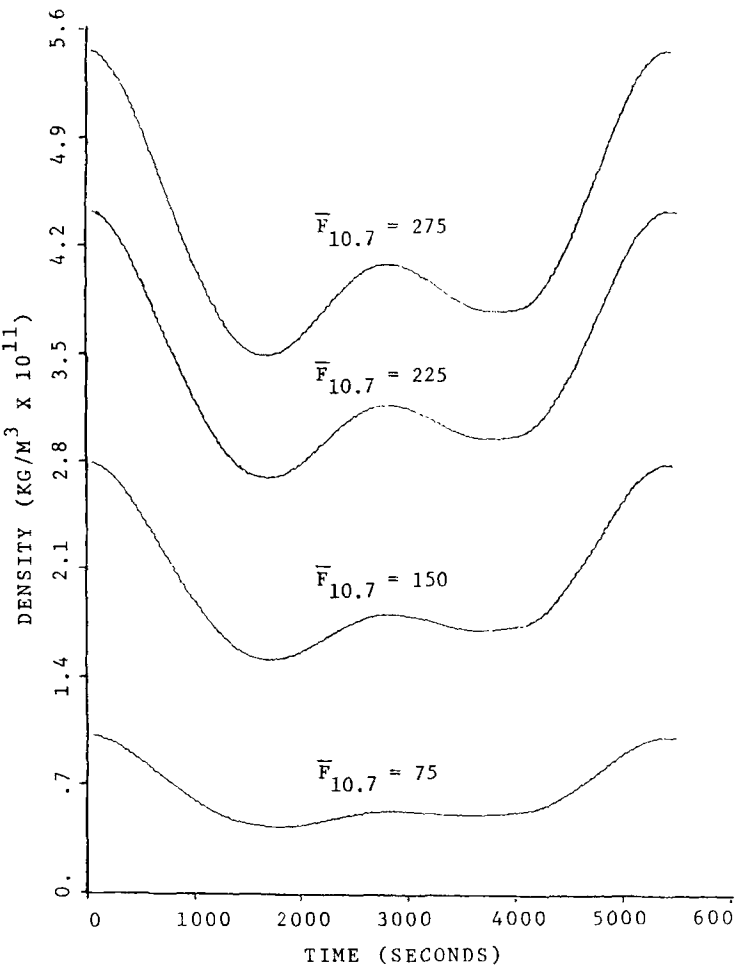

Fig. 6. Density profile variations due to changes in $\bar{F}_{10.7}$.

density versus time in this section. The trajectories were generated from the initial osculating elements:

$a = 6\,678\,155$ m

$e = 0.0$

$i = 67.99°$

$\omega = 3.02°$

$\Omega = 254.26°$

$E = 356.98°$

epoch $16^d2^h47^m55.537^s$ December 1973.

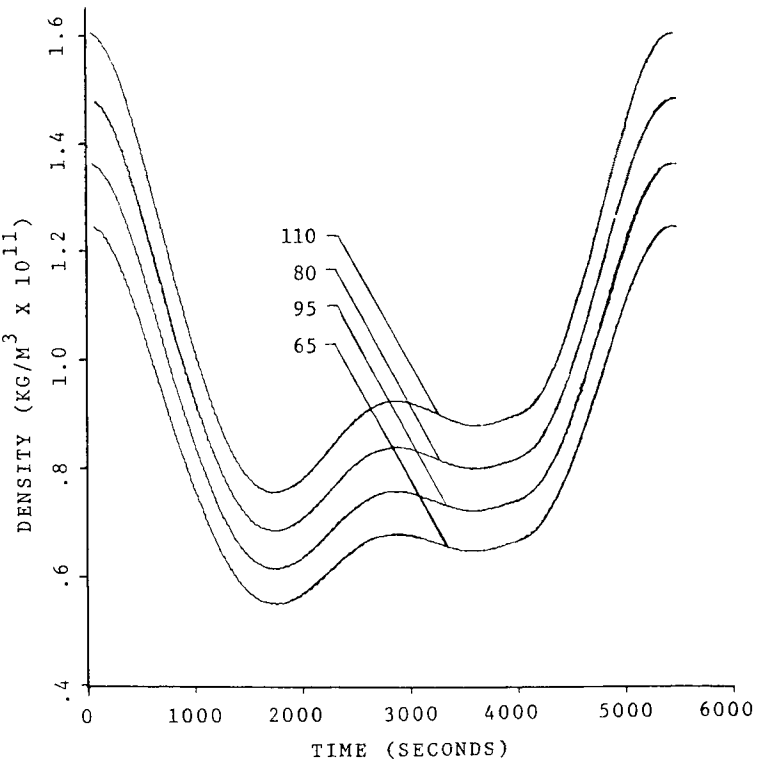

Fig. 7. Density profiles for values of daily $F_{10.7}$ about $\bar{F}_{10.7} = 85$.

The Newtonian equations of motion were numerically integrated by a fixed step size, third-order Runge–Kutta method with a ten-second step size. A single trajectory was generated and the various atmospheric density models were evaluated on this common trajectory. The force model for drag used densities from the Modified Analytic Jacchia–Roberts Model in the generation of the comparison orbit. The remaining modeled forces used to generate the comparison orbit were:

Two-body Geopotential: $\mu = 3.986\,013 \times 10^{14}\ \mathrm{m^3\ s^{-2}}$.

Nonspherical Earth: 1969 Smithsonian Standard Earth II to fourth order and fourth degree.

n-body: Solar and lunar gravitational perturbations based on Jet Propulsion Laboratory Development Ephemeris Number 19.

The density profiles shown in Figure 10 are those which would be modeled by various forms of the Modified Harris–Priester Model. The reference profile is the generating density profile modeled by the Modified Jacchia–Roberts Model, where

$$F_{10.7} = 75$$

$$\bar{F}_{10.7} = 75$$

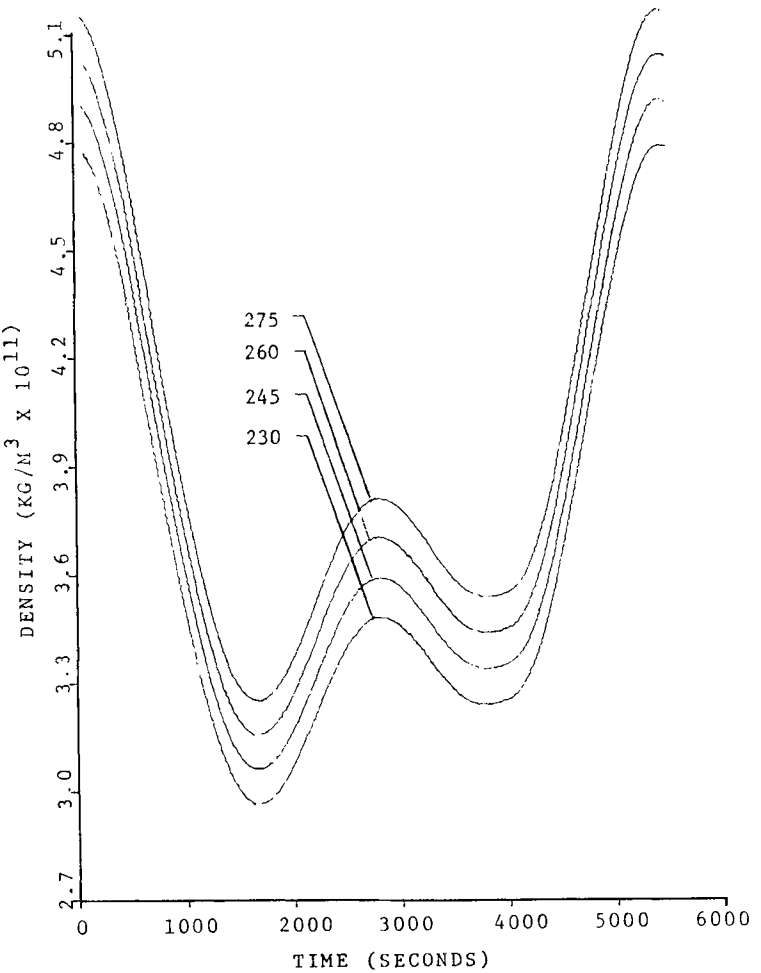

Fig. 8. Density profiles for values of daily $F_{10.7}$ about $\bar{F}_{10.7} = 250$.

and

$$K_p = 1 .$$

The other four profiles shown in Figure 10 are those density profiles which were computed by either the Modified Harris–Priester or Asymmetric Modified Harris–Priester models associated with $\bar{F}_{10.7} = 75$ where the shapes of the profiles shown were determined by setting the value of n in Equations (2) and (3) to either 3 or 6. The key to the symbols used to identify the curves in Figures 10 and 11 is given in Table I.

The density profiles shown in Figure 11 are similar to those in Figure 10 except that the values of $F_{10.7}$ and $\bar{F}_{10.7}$ used in the models is 275, a value representing the maximum extreme in the 11-year solar cycle. Close inspection reveals that the

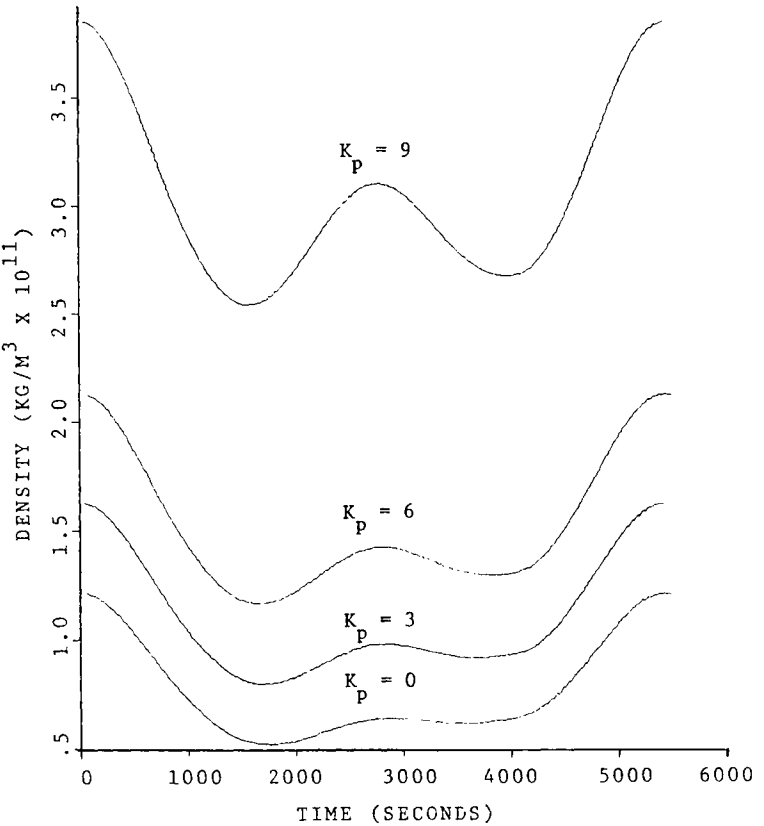

Fig. 9. Density profile variations due to changes in geomagnetic activity index.

density profiles determined by the Asymmetric Modified Harris–Priester Model with $n = 3$ most closely approximates the Jacchia–Roberts profile in shape. It appears that by judiciously scaling $\rho_{\min}$ and $\rho_{\max}$ in Equation (4), and by applying a small correction to n near the value $n = 3$, the Asymmetric Modified Harris–Priester profile will very nearly coincide with the Modified Jacchia–Roberts profile.

There is a systematic difference in the density profiles generated by the Jacchia–Roberts and Asymmetric Modified Harris–Priester Models which is not apparent in Figure 10. This difference is a result of the assumption by Jacchia [4] of a static temperature profile, whereas Harris and Priester used a dynamic temperature profile to generate their atmospheric density tables [7]. These differing approaches are manifested in the models through the temperature equations

$$\begin{aligned} T_D &= T_C(1 + R\cos^m \eta) \\ T_N &= T_C(1 + R\sin^m \theta) \end{aligned} \tag{5}$$

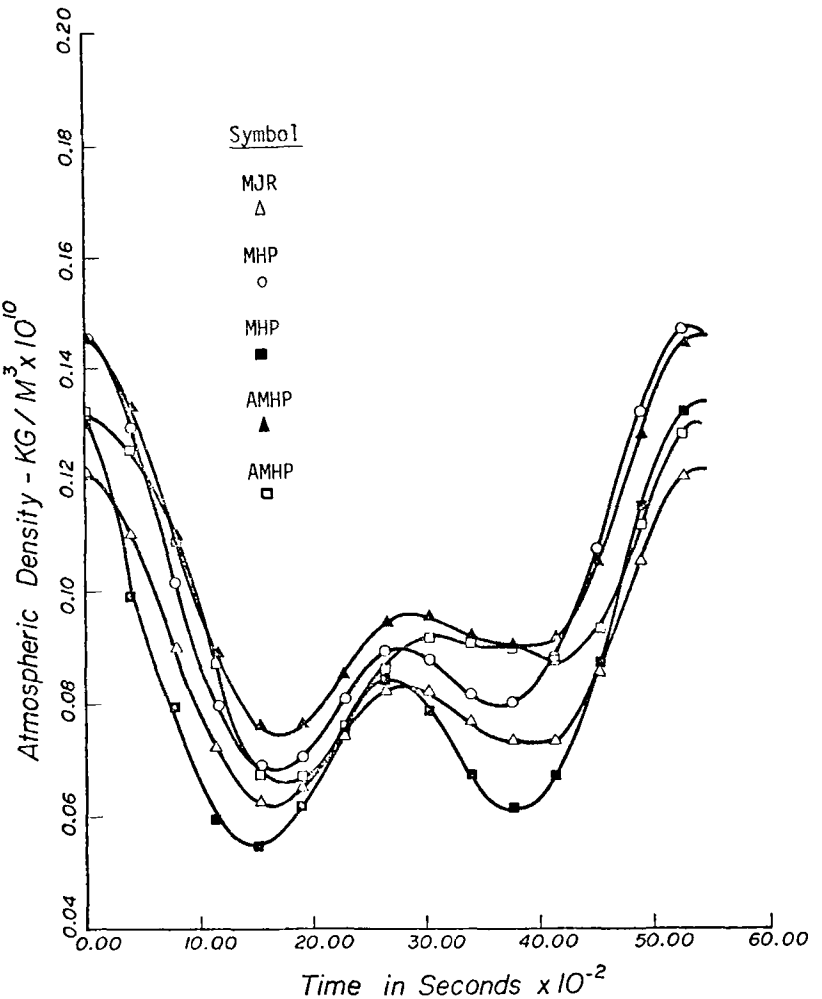

Fig. 10. Comparison of Jacchia–Roberts and Harris–Priester density profiles at low solar activity level.

TABLE I

Key to symbols in figures 10 and 11

Symbol	Definition
MJR △	Modified Jacchia–Roberts Analytical Model (Reference Model)
MHP ○	Modified Harris–Priester Model, $n = 3$
MHP ■	Modified Harris–Priester Model, $n = 6$
AMHP ▲	Asymmetric Modified Harris–Priester Model, $n = 3$
AMHP □	Asymmetric Modified Harris–Priester Model, $n = 6$

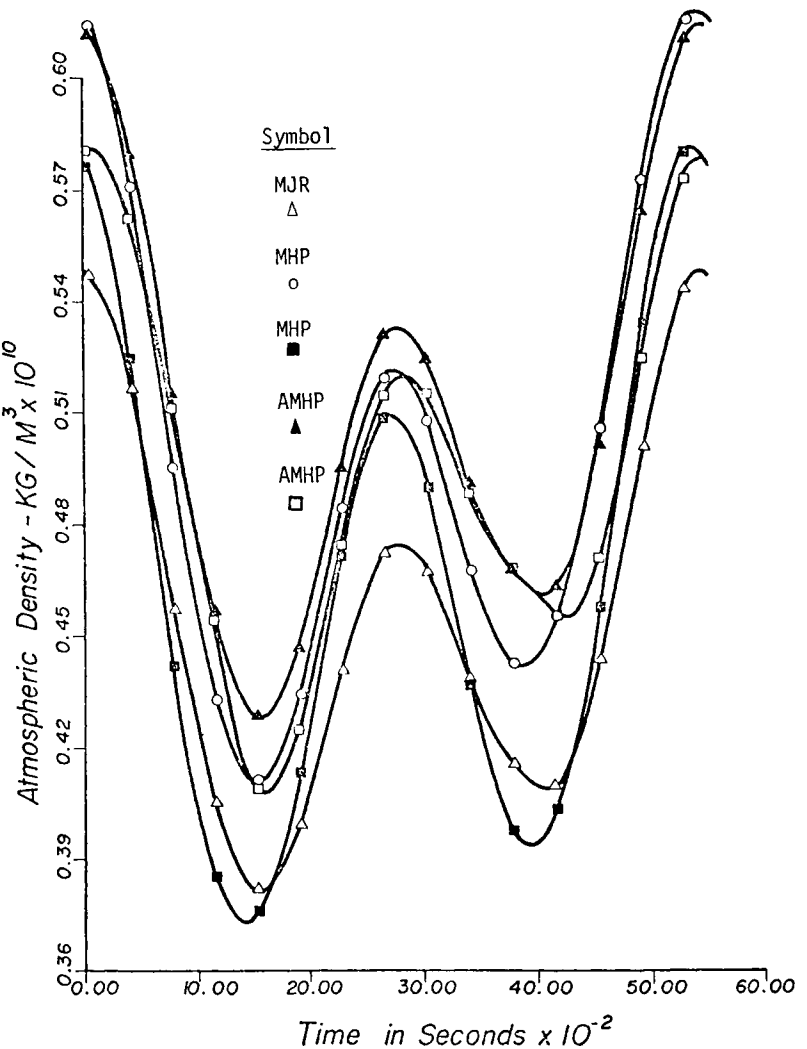

Fig. 11. Comparison of Jacchia–Roberts and Harris–Priester density profiles at high solar activity level.

in the Analytic Jacchia–Roberts Model and the density equations

$$\rho_D = \rho_{\min}(1 + Q \cos^m \eta)$$
$$\rho_N = \rho_{\min}(1 + Q \sin^m \theta) \tag{6}$$

in the Asymmetric Modified Harris–Priester Model. The quantity R appears as a constant in the former model whereas Q is given by

$$Q = (\rho_{\max} - \rho_{\min})/\rho_{\min} \tag{7}$$

which is not a constant valued quantity, in the latter model. The effect of this

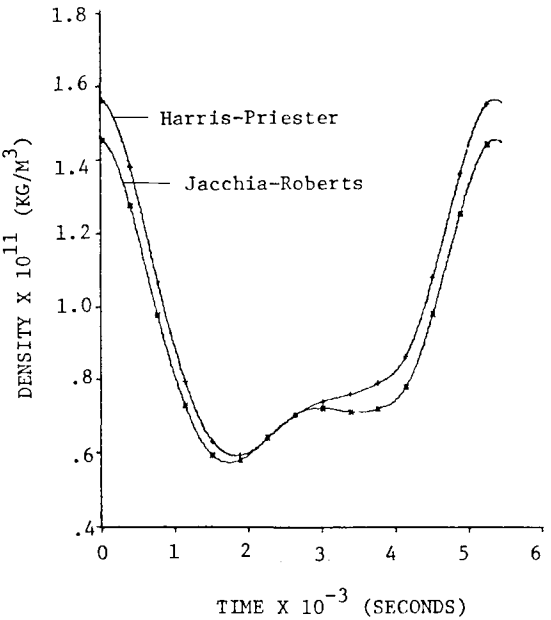

Fig. 12. Comparison of modified analytic Jacchia–Roberts density profile with asymmetric modified Harris–Priester density profile in a nearly circular orbit.

systematic difference in the two models is illustrated in Figure 12 which shows the density profiles generated by the Modified Analytic Jacchia–Roberts and Asymmetric Modified Harris–Priester Models during one orbital period along a trajectory with whose non-zero initial osculating Keplerian elements are:

$$a = 6\,682\,473.58 \text{ m}$$

$$e = 0.000\,646\,25$$

$$i = 68.0°.$$

The difference is most apparent between 3000 and 4000 s after the beginning of the orbit propagation. In this regard, the Asymmetric Modified Harris–Priester Model more accurately reflects the real world diurnal density variation than the Jacchia–Roberts Model.

Density profiles calculated by the U.S.S.R. Cosmos Satellite Derived Density Model are compared with the Modified Jacchia–Roberts profiles in Figures 13 and 14. The initial conditions for the generation of the comparison orbit are the same as those used for Figure 10. The pertinent parameters supplied to the models to generate the profiles in Figure 13 were

$$F_{10.7} = 79.1, F_{10.7} = 84.2, \text{ and } K_p = 1$$

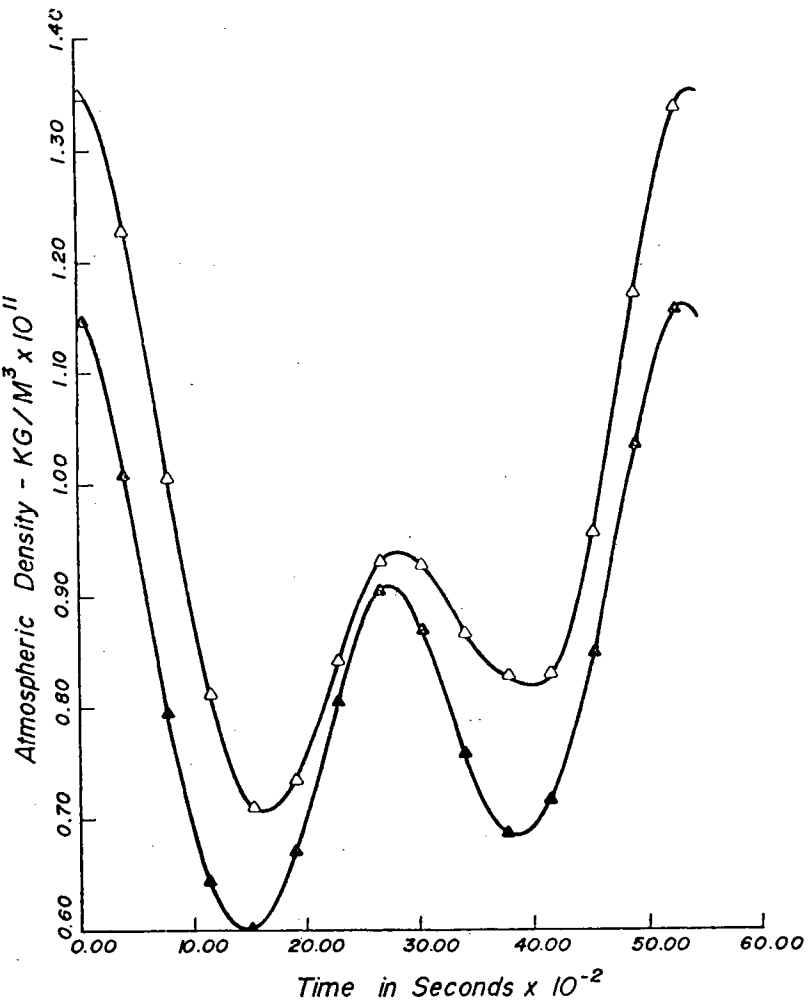

Fig. 13. Comparison of Jacchia–Roberts (△) and Russian (▲) density profiles at low solar activity level.

for the Jacchia–Roberts Model, and

$$F_{10.7} = 79.1, F_0 = 75, \text{ and } a_p = 4$$

for the U.S.S.R. Model. It should be noted that $K_p = 1$ and $a_p = 4$ are equivalent measures of geomagnetic activity. For the profiles shown in Figure 14, the defining parameters are

$$F_{10.7} = \bar{F}_{10.7} = 150, \text{ and } K_p = 1$$

for the Jacchia–Roberts profile, and

$$F_0 = F_{10.7} = 150, \text{ and } a_p = 4$$

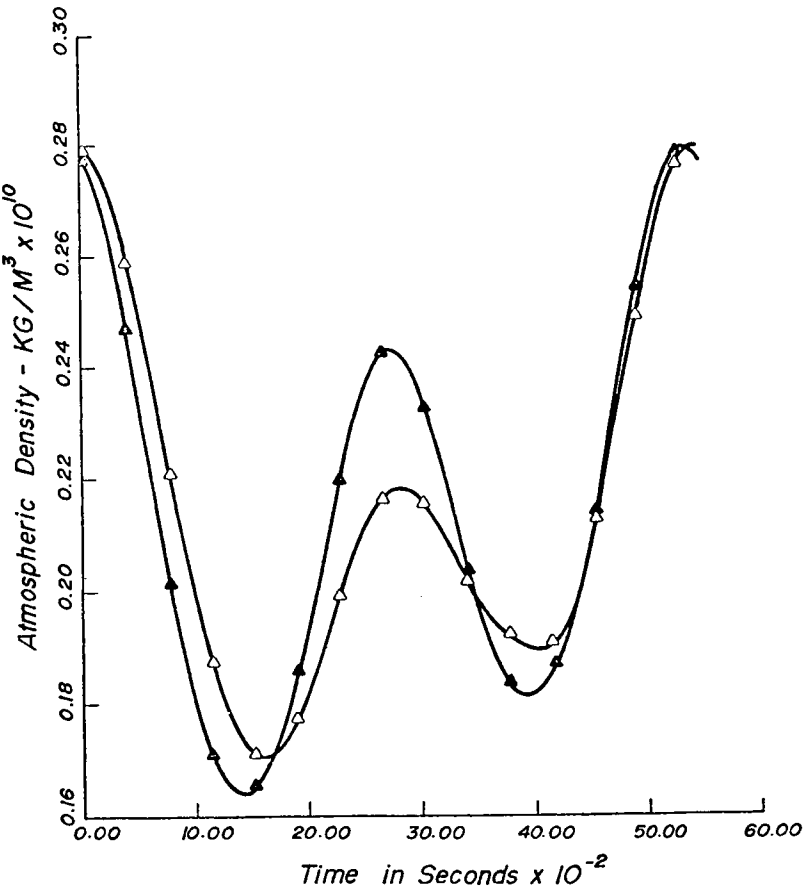

Fig. 14. Comparison of Jacchia–Roberts (△) and Russian (▲) density profiles at medium solar activity level.

TABLE II

Comparison of central processor (CP) time required for drag acceleration computation

Model	CP time for drag computations (s)	Total CP time for run[a] (s)
Analytic Jacchia–Roberts Model	20.34	58.77
Modified Analytic Jacchia–Roberts Model	15.97	54.61
Modified Harris–Priester Model	7.67	46.05
Russian Model	5.58	44.36

[a] Each run consisted of an integration of the equations of motion for approximately five periods in the circular orbit. The integrator was the fixed step third order Runge–Kutta with Ralston's coefficients. The step size was 25 s.

for the U.S.S.R. profile. The density profiles in these cases are similar in some sense, but not as much so as the Asymmetric Modified Harris–Priester profiles.

7. Computational Characteristics of the Models

Comparison of the time required to compute the model densities is shown in Table II. In terms of computational speed, the U.S.S.R. is the most efficient model, with the Modified Harris–Priester Model following closely. It should be noted that there is practically no difference in the computation time between the Modified and Asymmetric Modified Harris–Priester Models. The Analytic Jacchia–Roberts Model requires much more time than either the Harris–Priester or the U.S.S.R. model. Even though the modification of the Jacchia–Roberts Model proposed in [2] reduces the time requirements by over 20%, the other models are still more than twice as fast.

In the Analytic Jacchia–Roberts Model, the barometric differential equation is integrated by the method of partial fractions. To accomplish this, the roots of a fourth degree polynomial must be determined where it is known that the polynomial has two real and unequal roots and two complex roots. The nature of the polynomial is such that convergence to the roots with a Newton–Raphson iteration cannot be assured to a tolerance of less than 1×10^{-4} when computations are accomplished with a computer which carries 14 significant digits. When double precision arithmetic is used, the tolerance can be reduced to 1×10^{-18}. The result of not determining the roots of the polynomial to a small enough tolerance is that occasionally the density increases with an increase in altitude. This characteristic is illustrated by the densities calculated at the beginning of each integration step of a simulated satellite orbit shown in Table III.

TABLE III

Sample density profile determined by the analytic Jacchia–Roberts Model using single precision arithmetic

Altitude (M)	Density $KG\,M^{-3} \times 10^{11}$
300 000.01	2.165 16
300 001.53	2.163 38
300 006.65	2.166 73
300 015.38	2.166 70
300 027.70	2.161 65
300 043.60	2.159 15
300 063.09	2.159 88
300 086.14	2.160 69

In an independent study, Botbyl [9] investigated the sensitivity of the density calculation to the evaluation of a fifth-order polynomial occurring in the Analytic Jacchia–Roberts algorithm. For computations on the CDC 6400/6600 at the

University of Texas at Austin, Botbyl showed that perturbing the coefficient of the fifth order term by 1 in the 14th digit resulted in density calculations accurate to no more than two or three digits. However, the reference density used for comparison did not consider the errors due to inaccurate determination of the roots discussed above. To resolve the question of the computational accuracy of the model, three density-vs-altitude profiles were determined with (1) all single precision arithmetic, (2) double precision computation of the polynomial and single precision arithmetic otherwise, and (3) all double precision arithmetic. The density digits for the three profiles are shown in Table IV. In general, it can be seen that the single precision computation is accurate to three or four digits and that computing only the polynomial with double precision arithmetic does not significantly increase the accuracy of the computation. The importance of the increase in accuracy achieved by performing the density calculations in double precision must be weighed against the increase in computation time and core storage requirements.

TABLE IV

Comparison of density calculations with the analytic Jacchia–Roberts Model

Altitude (kM)	Single precision	Density digits double precision Equation (A. 12h) single precision all other calculations	Double precision
90	3.46	3.46	3.46
100	5.4952	5.4956	5.4977
150	2.5798	2.5800	2.5809
200	3.9305	3.9308	3.9322
400	8.0247	8.0253	8.0283
600	4.2362	4.2365	4.2381
800	3.8025	3.8028	3.8042
1000	8.8327	8.8333	8.8366
1500	1.5922	1.5923	1.5929
Central processor time (s)	0.289	0.292	0.376
Central memory core storage (words)	12000_8	12700_8	15300_8

It has been mentioned previously that the Modified Analytic Jacchia–Roberts Model is approximately 20% faster than the unmodified version. A representative comparison of the densities calculated by the modified and the unmodified models using single precision arithmetic is shown in Table V. Further comparison densities were computed for T_∞ ranging from 800 K to 2000 K. The largest error encountered was 0.08% which occurred at an altitude of 125 km when $T_\infty = 2000$ K. Between the altitude of 90 and 100 km the unmodified and modified algorithms are identical. The

TABLE V

Comparison of densities calculated by the analytic Jacchia–Roberts Model and the modified analytic Jacchia–Roberts for $T_\infty = 1100$ K

	Atmospheric density digits		
Altitude (km)	Unmodified model	Modified model	Percent error
100	5.497 742 3	5.497 754 7	0.0002
110	9.930 300 6	9.930 322 9	0.0002
120	2.459 633 9	2.459 639 4	0.0002
125	1.401 830 3	1.401 820 2	0.0007
200	2.938 129 0	2.937 956 2	0.0058
300	2.786 664 6	2.786 375 4	0.0104
400	4.876 186 1	4.875 585 2	0.0123
500	1.041 629 2	1.041 496 1	0.0128
750	3.621 325 2	3.621 006 1	0.0088
1000	4.421 350 8	4.421 498 2	0.0033
1500	7.659 732 6	7.660 369 9	0.0083

Modified Analytic Jacchia–Roberts Model then is at least as accurate, and most of the time is more accurate than the basic algorithm when using single precision arithmetic.

The Modified Harris–Priester Model is a very simple, straightforward method which displays no computational idiosyncracies. However, potential users of the model should consider the physical interpretation of Equation (3) which shapes the density profile with respect to the diurnal density variation. The value of the exponent n could be any real number. Common sense, however, tell us that certain values of n would produce profiles that almost certainly are not physically realizable. It is not improbable that the density variation due to diurnal heating is a smooth process, that is to say at least continuously differentiable. The diurnal variation given by the Modified Harris–Priester Model would be smooth when $n > 1$ so that $n = 1$ is an absolute lower bound. However, for values $1 < n \leq 2$, the modeled diurnal variation would be such that the profile is broader around the maximum than the minimum and this characteristic opposes the observed character of the diurnal variation [8]. Conversely, when n is large (greater than 8), the density profile becomes too sharp near the diurnal maximum. The curves shown in Figure 15 of $\cos^n(\psi/2)$ for various values of n show that the changes in the shape of the curve are large for small changes in n when $2 \leq n \leq 8$ and the shape changes very little with n when $n > 8$. The point to be made here is that when a powered cosine function is to be used to describe the diurnal density variation, the exponent should be limited to values between 2 and 8. Indeed, Jacchia has consistently arrived at exponents in this range [5, 8, 10, 11, 12].

The U.S.S.R. Model is also a simple, straightforward algorithm. It is very fast and relatively sophisticated; however, its use is limited to the altitude band from 140 km to 500 km and to solar flux levels from 65 to 165×10^{-22} W m^{-2} Hz^{-1}. Furthermore,

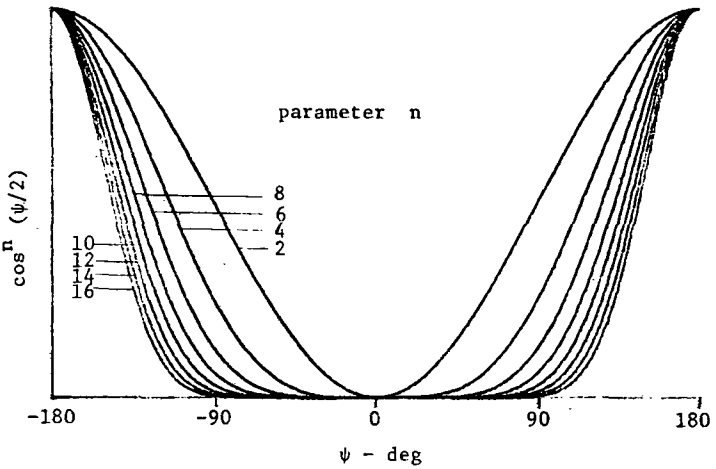

Fig. 15. Effect of n on $\cos^n(\psi/2)$.

certain conditions can cause the model to yield negative densities. These conditions, which are physically realizable, occur when the 6-month average of the daily $F_{10.7}$ is near enough to 150×10^{-22} W m^{-2} Hz^{-1} that $F_0 = 150$ is chosen as the reference flux. The scale factor K_1 which corrects the density for short term fluctuations in solar activity becomes negative for values of the daily $F_{10.7}$ and altitudes below the curve shown in Figure 16. It is true that the conditions for which K_1 becomes non-positive are not likely to occur often, but variations in $F_{10.7}$ of the magnitude of 75×10^{-22} W m^{-2} Hz^{-1} have occurred and the potential user should be aware of this limitation in the model. The other factors are always positive in the altitude region between 140 and 500 km.

The Jacchia–Roberts models are the most sophisticated of the models considered and they provide upper atmosphere density values over the greatest range of altitudes. The Jacchia–Roberts models and the U.S.S.R. Model provide corrections

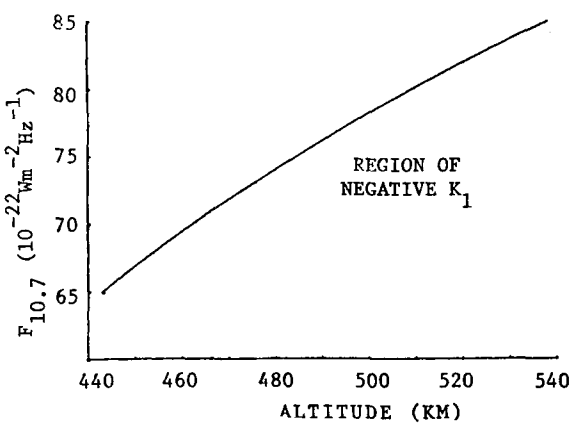

Fig. 16. Curve of $K_1 = 0$ for $F_0 = 150$.

for the diurnal variation, variations in solar activity over both the 11-year and 27-day cycles, semiannual variation, and for variations in geomagnetic activity. In addition, the Jacchia–Roberts models account for seasonal-latitudinal variations in the assumed constant boundary condition at 90 km and seasonal latitudinal variations in helium concentrations. The Modified and Asymmetric Modified Harris–Priester Model accounts for only the diurnal variation and the variation in density due to the variation of solar activity over the 11-year solar cycle. It should be remembered that the original model given by Harris and Priester [7] does include procedures for accounting for all of the variations discussed herein. However, one of the fundamental motives in this investigation was the determination of an efficient model which can be adapted to model 'real-time' atmospheric density variations and the Asymmetric Modified Harris–Priester Model has the desired characteristics of computational efficiency and adequate fidelity in representing the diurnal variation to form the base for such an adaptive model. The details of the formulation of such an adaptive model are given in [6].

8. Conclusions

In the previous discussions comparisons of the computational aspects of the models have been made. In general, all of these models can be said to be quasi-dynamic representations of the atmospheric density; that is, they are neither completely static nor completely dynamic. The time dependent variations in the model density profiles are determined by both the evaluation of explicit continuous functions of time and by the input of time varying parameters to the algorithms. These input parameters, specifically measured values of solar and/or geomagnetic activity, are available for use by the algorithms in discrete form only. Solar activity is reported as 1-day averages and geomagnetic activity is available every 3 hr. Since the time delay between the measurement of a change in geomagnetic activity and the corresponding response in the atmospheric density is approximately 6.7 hr, a direct data link with the geomagnetic activity index reporting agency would be required for real time or near real time applications.

References

[1] Roberts, C. E., Jr.: 1971, 'An Analytical Model for Upper Atmosphere Densities based upon Jacchia's 1970 Models', *Celes. Mech.* **4**, 368.

[2] Wagner, W. E. and Velez, C. E.: 1972, 'Goddard Trajectory Determination Subsystem Mathematical Specifications', NASA Goddard Spaceflight Center.

[3] Elyasberg, P. E., Kugaenko, B. V., Synitsyn, V. M., and Voskovsky, M. I.: 1972, 'Upper Atmosphere Density Determination from the Cosmos Satellite Deceleration Results', *Space Res.* **XII**, 727.

[4] Jacchia, L. G.: 1970, 'New Statis Models of the Thermosphere and Exposphere with Empirical Temperature Profiles', Smithsonian Astrophysical Observatory, Special Report No. 313.

[5] Jacchia, L. G.: 1971, 'Revised Static Models of the Thermosphere and Exosphere with Empirical Temperature Profiles', Smithsonian Institution, Astrophysical Observatory, Special Report No. 332.

[6] Dowd, D. L.: 1977, 'Adaptive Estimation of Atmospheric Drag on Near Earth Earth Satellites', Institute for Advanced Study in Orbital Mechanics, Technical Report 77-4, The University of Texas at Austin, Austin, Tex., U.S.A.
[7] Harris, I. and Priester, W.: 1965, 'Atmospheric Structure and Its Variations in the Region from 120 to 800 km', COSPAR International Reference Atmosphere (CIRA).
[8] Jacchia, L. G. and Slowey, J.: 1967, 'The Shape and Location of the Diurnal Bulge in the Upper Atmosphere', *Space Res.* **VII**, 626.
[9] Botbyl, G. W.: 1973, 'Technical Note on Expected Significance Using Subroutine ATDENS', Department of Aerospace Engineering and Engineering Mechanics, The University of Texas at Austin, Tex., internal memorandum.
[10] Jacchia, L. G.: 1960, 'A Variable Atmospheric Density Model from Satellite Accelerations', Smithsonian Institution Astrophysical Observatory Research in Space, Special Report No. 39.
[11] Jacchia, L. G., Campbell, I. G., and Slowey, J. W.: 1973, 'A Study of the Diurnal Variation in the Thermosphere as Derived by Satellite Drag', *Planetary Space Sci.* **21**, 1825.
[12] Jacchia, L. G.: 1965, 'Satic Diffusion Models of the Upper Atmosphere with Empirical Temperature Profiles', Smithsonian Contributions to Astrophysics, Vol. 8, No. 9.